Available online at www.sciencedirect.com
SCIENCE DIRECT®
International Journal of Heat and Mass Transfer 47 (2004) 4721–4731
International Journal of HEAT and MASS TRANSFER
www.elsevier.com/locate/ijhmt

Experimental investigation on the heat transfer characteristics of axial rotating heat pipes

F. Song, D. Ewing, C.Y. Ching *

Department of Mechanical Engineering, McMaster University, Hamilton, ON, Canada L8S 4L7

Received 13 October 2003; received in revised form 27 May 2004
Available online 20 July 2004

Abstract

The heat transfer performance of axial rotating heat pipes was measured under steady state at rotational speeds up to 4000 RPM, or a maximum centrifugal acceleration of 170g, and heat transfer rates up to 0.7 kW. A cylindrical and an internally tapered heat pipe with water as the working fluid were tested with different fluid loadings that ranged from 5% to 30% of the total interior volume. The measurements were used to characterize the effects of rotational speed, working fluid loading, and heat pipe geometry on the heat transfer performance. The internal taper on the condenser was found to significantly increase the heat transfer rate compared to the cylindrical case. A comparison between the test results and predictions from previous models showed that natural convection in the liquid film at the heat pipe evaporator plays an important role in the heat transfer mechanism at high rotational speeds.

Keywords: Axial rotating heat pipe; Heat transfer characteristics; Working fluid loading; Heat pipe geometry

1. Introduction

Rotating heat pipes are highly effective two-phase heat transfer devices that utilize the centrifugal force produced by the rotation to drive the working fluid in these devices [1]. The heat transfer through the heat pipe is achieved by evaporating the working fluid in a high-temperature evaporator section, and then condensing it in a lower temperature condenser section (Fig. 1). Rotating heat pipes can be classified as radial or axial depending on the configuration of the heat pipe relative to the direction of rotation or the centrifugal force. In radial rotating heat pipes, the evaporator and condenser are separated in the radial direction so the centrifugal force is parallel to the liquid flow to drive the liquid condensate from the condenser to the evaporator. In axial rotating heat pipes, studied here, the evaporator and condenser are separated in the direction parallel to the axis of rotation so the centrifugal force is normal to the heat pipe axis. The liquid flow is driven by a hydrostatic pressure gradient in the film caused by the centrifugal force in a cylindrical heat pipe as shown in Fig. 1(a), or by the component of the centrifugal force parallel to the liquid flow if a taper is used on the inner surface as shown in Fig. 1(b). In both cases, the vapor flow is driven by a pressure difference in the vapor that develops between the evaporator and condenser.

A number of investigations have shown that in most cases the heat transfer is determined by the thermal resistance associated with the phase changes in the evaporator and condenser. For low rotational speeds or more properly low centrifugal accelerations, the gravitational force has an effect on the distribution of the liquid film so that in the horizontal orientation the film is not uniform around the heat pipe inner surface. However, when the centrifugal acceleration is greater than approximately 20 times gravity (i.e., $a/g > 20$), the centrifugal force becomes more dominant and the liquid film on the inner surface is approximately annular for all

* Corresponding author. Tel.: +1-905-525-9140; fax: +1-905-572-7944.
E-mail address: chingcy@mcmaster.ca (C.Y. Ching).

0017-9310/$ - see front matter © 2004 Elsevier Ltd. All rights reserved.
doi:10.1016/j.ijheatmasstransfer.2004.06.001

Nomenclature

a	centrifugal acceleration [m s^{-2}]
c_p	specific heat at constant pressure [J kg^{-1} K^{-1}]
g	gravitational acceleration [m s^{-2}]
L	heat pipe length [m]
$\dot{m}$	mass flow rate [kg s^{-1}]
N	rotational speed [RPM]
Q	heat transfer rate [W]
R	heat pipe inner radius [m]
R_l	liquid film thermal resistance [K W^{-1}]
T	temperature [K]
α	taper angle [°]
γ	fluid loading ratio
ρ	density [kg m^{-3}]
ω	angular velocity [rad s^{-1}]

Subscripts

c	condenser
e	evaporator
i	inlet
l	liquid
o	outlet
w	heat pipe wall

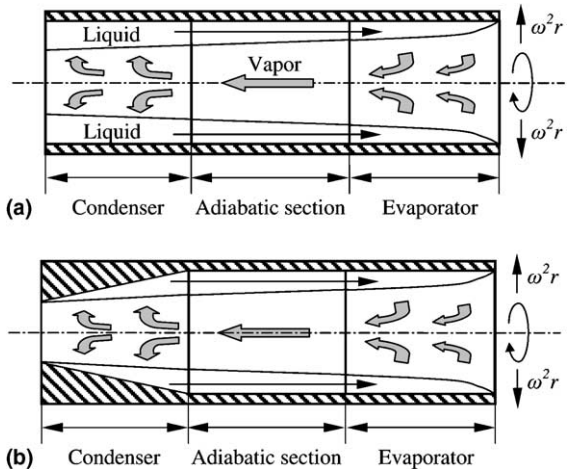

Fig. 1. Schematic of rotating heat pipe and typical geometry of (a) a cylindrical heat pipe and (b) a condenser-tapered heat pipe.

orientations [2]. In these cases, the phase change in the condenser has been modeled using a modified Nusselt film condensation model for either a tapered [3] or a cylindrical [4] condenser. Measurements performed by Daniels and Al-Jumaily [3] and Vasiliev and Khrolenok [5] for the condenser heat transfer at centrifugal accelerations from 20g to 200g were in good agreement with the predictions of this model. Marto and coworkers [6–8] performed a series of experiments in the rotational speed range 700–2800 RPM or a/g of 7–160 that showed the thermal resistance of the condenser of tapered heat pipes was less than half that of the cylindrical case. Ponnappan et al. [9] performed measurements using tapered heat pipes at much higher rotational speeds of 5000–30,000 RPM ($200 < a/g < 7350$), and found the modified Nusselt film condensation model [3] over predicted their measurements by approximately a factor of 4. Song et al. [10] later attributed this discrepancy to the large fluid loading in the heat pipes tested by Ponnappan et al. [9]. In particular, they found that small amounts of excess fluid pools in the evaporator, but as the fluid loading is increased it affects the film thickness in the condenser. Song et al. [10] showed that the predictions of the modified Nusselt film condensation model were in reasonable agreement with the measurements of the condenser heat transfer by Ponnappan et al. [9] when the effect of fluid loading was considered.

There have been fewer investigations to characterize the evaporator performance in rotating heat pipes. For low and modest rotational speeds, the phase transformation occurs through nucleate boiling that has a smaller thermal resistance relative to the film condensation process. At high rotational speeds ($a/g > 100$), Judd and Merte [11] and Ulucakli and Merte [12] found that nucleate boiling was suppressed in pool boiling and natural convection was increased. Vasiliev and Khrolenok [5] found similarly that nucleate boiling tended to be suppressed and natural convection became more important in the evaporator of a rotating heat pipe as the centrifugal acceleration increased from 20g to 200g. It should be noted that Vasiliev and Khrolenok [5] were characterizing the performance of a rotating heat pipe with a large step change in the heat pipe inner diameter between the adiabatic and evaporator sections. As a result, the heat transfer at the evaporator was similar to pool boiling. Song et al. [10] showed that when the suppression of boiling was considered for high rotational speeds, the thermal resistance of the evaporator became a significant part of the overall thermal resistance of the heat pipe and thus, should be considered when predicting the overall heat transfer performance of the rotating heat pipe.

Most previous models for cylindrical and tapered rotating heat pipes, however, have considered only the condenser heat transfer and neglected the thermal

resistance at the evaporator. This is only reasonable when the evaporator is operating in the nucleate boiling regime. Vasiliev and Khrolenok [5] proposed a complete model for the stepped heat pipe but considered the condenser and evaporator as discrete components that made it not applicable to heat pipes without a step. Li et al. [13] developed a film evaporation model that was analogous to the modified Nusselt film condensation model, and coupled this evaporator model with the film condensation model [3] to predict the heat transfer performance of a tapered heat pipe. More recently, Song et al. [10] developed a model that included a mixed convection film evaporation model in the evaporator. In this case, the heat was transferred across the film by both conduction and natural convection, so that it reduced to Li et al.'s model if natural convection was negligible. The predictions from Song et al.'s model [10] indicate the thermal resistance of the evaporator is on the same order as the condenser in many high-speed rotating heat pipe applications. In many cases, the predicted thermal resistance for the overall heat pipe was significantly less than that predicted by Li et al. [13].

Heretofore, however, there have only been limited experiments on the overall performance of rotating heat pipes [3,9] that could be used to examine if the model proposed by Song et al. [10] could accurately predict the performance of high-speed axial rotating heat pipes. The predictions of heat transfer from Song et al.'s model were in reasonable agreement with the experimental measurements of Daniels and Al-Jumaily [3] and Ponnappan et al. [9], though they were unable to explain the slight decrease in the measured heat pipe performance with rotational speed found by Ponnappan et al. [9]. Further, unlike previous models, Song et al.'s model [10] could be used to examine the effect of different fluid loadings in the heat pipe by assuming an annular liquid film at high rotational speeds ($a/g > 20$). They found that the optimum fluid loading in the rotating heat pipe predicted by the model varies significantly with rotational speed and heat flux. This is different from the findings of Nakayama et al. [14] that at low rotational speeds ($a/g < 13$) the liquid should fill approximately 10–14% of the heat pipe interior volume.

The objective of this study was to experimentally investigate the performance of axial rotating heat pipes and assess the models of Li et al. [13] and Song et al. [10]. Measurements were performed for a cylindrical and a 2° tapered condenser heat pipe with different fluid loadings at rotational speeds from 2000 to 4000 RPM, that correspond to a/g of 42–170.

2. Experimental facilities and methodology

The rotating heat pipe was driven using a Toshiba EQP3 motor with a VFS9S controller capable of rotational speeds up to 4775 RPM. The motor was directly connected to the condenser end of the heat pipe using a plastic ODG Bowex flexible coupling. The heat pipe was supported at the adiabatic section using a 3 mm thick, 178 mm long Teflon sleeve in a stainless steel tube. This tube was mounted in two self-aligning bearings, such that the ends of the Teflon sleeve were 10 mm away from the nominal start of the condenser and evaporator sections. A cooling water jacket was used to remove the heat from the condenser, while two different methods were used to heat the evaporator. In the first configuration, shown in Fig. 2(a), the heat was added to the evaporator of the heat pipe using an induction heating coil. It was, however, found that the induction heating of the surrounding metal plate was a significant portion of the total electrical power making it difficult to accurately determine the heat flux into the evaporator heating coil, and obtain an energy balance for the heat pipe. The heat transfer rate could only be determined by applying an energy balance to the condenser water jacket. In order to evaluate the accuracy of the measurements of heat transfer from the condenser, the performance of one rotating heat pipe was also characterized using a second configuration with a heating water jacket at the evaporator shown in Fig. 2(b). In this case, the maximum temperature at the evaporator was limited by the heating water temperature, so that it was not possible to perform measurements for high heat transfer rates when the rotational speed was low. Thus, most of the measurements reported in this paper were performed using the first configuration with the evaporator induction heating.

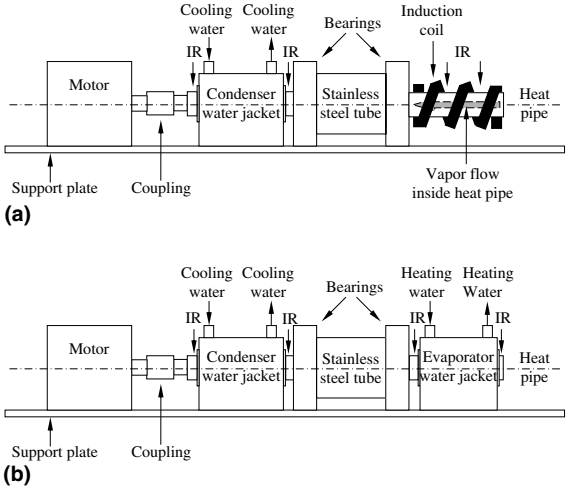

Fig. 2. Schematic of the high-speed rotating heat pipe test facility configured with (a) induction heating at the evaporator and water jacket at the condenser and (b) water jackets at the evaporator and condenser.

In the first configuration, a Radyne 3 kW induction heating system was used to supply heat to the evaporator section. The induction coil was water cooled and the energy extracted from the coil was determined by measuring the flow rate and temperature change of water across the cooling system. The coil was positioned to surround the entire rotating evaporator so that a nearly uniform heat flux could be achieved at the evaporator. The wall temperature distribution along the evaporator was measured in the gaps between the coils using a Raytec infrared (IR) thermometer mounted above the heat pipe.

The cooling water jacket at the condenser was 103 mm long with a 19 mm annular gap between the stationary Teflon shell and the rotating heat pipe (Fig. 3). The two ends of the water jacket were sealed using 25 mm diameter CR bore seals mounted into the Teflon block. The water flow entered and exited the water jacket through 6.4 mm holes on the top of the channel, with centers located 16 mm from the two ends of the channel. The inlet and outlet temperatures of the cooling water were measured using T-type thermocouples with an overall accuracy of ±0.5 °C. The wall temperature of the condenser was measured at both ends just outside of the water jacket using the IR thermometer as shown in Fig. 3. The cooling water was supplied using the closed loop system shown in Fig. 4. The flow rate was controlled using a valve and by-pass leg that circulated a portion of the flow from the pump back to the reservoir. The remainder was circulated through the water jacket and the volume flow rate was measured using a rotameter with an accuracy of ±2% of full scale. The flow exiting the cooling water jacket passed through the recuperator and returned to the reservoir.

The heat transfer rate from the condenser was evaluated as

$$Q_c = \dot{m}_{l,c} c_p (T_{c,o} - T_{c,i}), \quad (1)$$

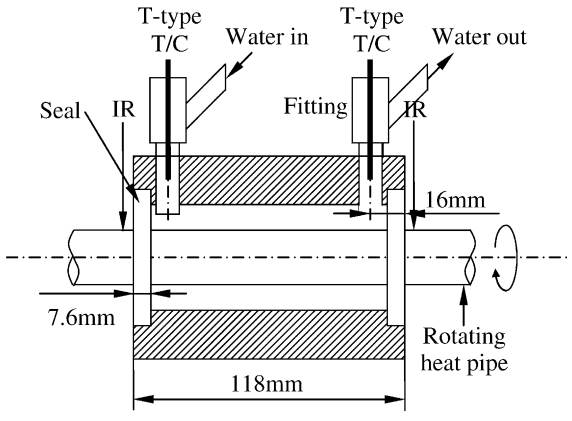

Fig. 3. Schematic of the water jacket at the condenser.

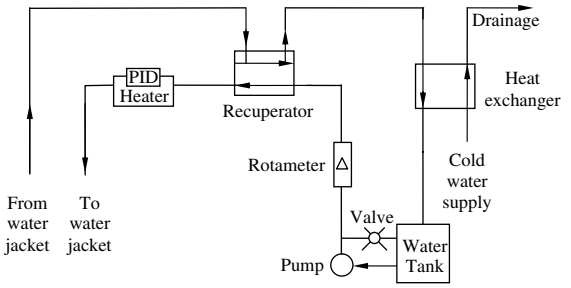

Fig. 4. Schematic of the closed loop heating/cooling system.

where $\dot{m}_{l,c}$ is the mass flow rate of water, and $T_{c,i}$ and $T_{c,o}$ are the inlet and outlet water temperature of the water jacket. For the measurements here, a large water flow rate was desirable to enhance the convection heat transfer between the water flow and the rotating heat pipe in order to maintain a relatively isothermal boundary condition at the condenser. The volume flow rate was 1.4–2.0 $1\,min^{-1}$ that yielded temperature differences in the cooling water of 2–6 °C. The uncertainty of the heat transfer measurement estimated following the approach of Coleman and Steele [15] was ±15% at 95% confidence for heat transfer rates of 0.5–0.7 kW, and up to ±50% at 95% confidence for the lowest heat transfer rates of 0.1–0.2 kW. In order to better evaluate the uncertainty in the heat transfer measurements, experiments were performed for one rotating heat pipe using the second configuration of water jackets at the condenser and evaporator so the energy balance of the system could be verified. The heating water jacket at the evaporator was similar to that at the condenser but 10 mm shorter to leave enough space on both ends of the evaporator to measure the wall temperature with the IR thermometer. In this configuration, the water flow to the evaporator water jacket was supplied using the closed loop system shown in Fig. 4. A 2 kW heater with a PID controller was used to maintain the water entering the jacket at a constant temperature. The flow rate was set to 1.2 $1\,min^{-1}$ and the temperature change in the water across the evaporator was in the range 3–7 °C. The uncertainty in the heat transfer varied from ±15% to ±35% at 95% confidence. The water flow to the condenser jacket in this instance was supplied from the city supply and measured using a rotameter with an accuracy of ±2% of the reading.

A cylindrical and an internally tapered condenser heat pipe (Fig. 1) with distilled water as the working fluid were tested at rotational speeds of 2000–4000 RPM, and heat transfer rates of 0.1–0.7 kW. The dimensions of the heat pipes and the different fluid loadings used in the current tests are summarized in Table 1.

Table 1
Specifications of the rotating heat pipes

	Cylindrical heat pipe	Tapered heat pipe
Evaporator length	121 mm (4.75 in.)	
Adiabatic length	184 mm (7.25 in.)	
Condenser length	102 mm (4.0 in.)	
Evaporator taper	0°	
Adiabatic taper	0°	
Condenser taper	0°	2°
Heat pipe wall material	Copper	
Heat pipe outer diameter	25.4 mm (1.0 in.)	
Wall thickness at condenser end	3 mm (0.125 in.)	6 mm (0.25 in.)
Wall thickness at evaporator end	3 mm (0.125 in.)	2.8 mm (0.11 in.)
Working fluid	Distilled water	
Working fluid charge (mass/percentage of the interior volume filled with liquid)	6.3*g*/5.5% 18.2*g*/15.9%	9.2*g*/9.1% 18.2*g*/18.0% 32.0*g*/31.7%

3. Experimental results

The heat transfer performance of the tapered heat pipe with 9.2*g* of water was initially characterized with the water jacket at the evaporator. The heat transfer rates into the evaporator (Q_e) and out of the condenser (Q_c) were in good agreement, with the average difference being less than 5% (Fig. 5). This is true at all the heat transfer rates suggesting that the error in the measurements was smaller than that estimated by the uncertainty analysis. The inlet water temperature of the condenser cooling jacket varied from 15 to 18 °C in these measurements, and the average condenser wall temperature varied from 26 to 30 °C. The evaporator wall temperature measured with the IR thermometer at the ends of the heating jacket ranged from 37 to 59 °C for the different heating conditions, with the temperature difference along the evaporator being less than 4.0 °C.

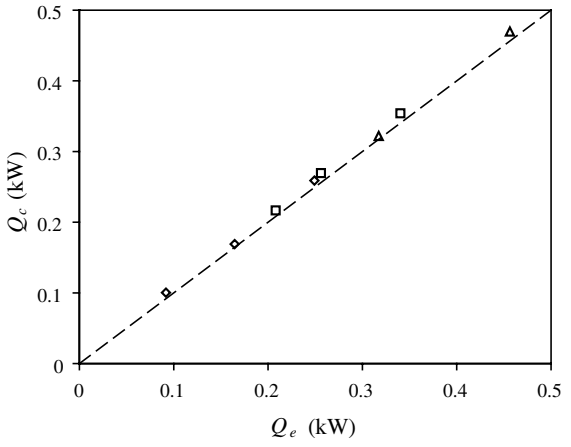

Fig. 5. Comparison of the heat transfer rates determined at the condenser and evaporator water jackets for the tapered heat pipe with 9.2*g* of water at (◇) 2000 RPM, (□) 3000 RPM, (△) 4000 RPM.

The heat transfer performance of this heat pipe was also measured using the induction coil at the evaporator. The inlet temperature of the water in the condenser cooling jacket varied from 19 to 28 °C in this case, and the average condenser wall temperature varied from 26 to 38 °C. The wall temperature difference along the evaporator measured between induction coils with the IR thermometer was less than 1.5 °C, indicating a nearly uniform evaporator temperature. A comparison of the heat transfer performance measured from both configurations is shown in Fig. 6 for rotational speeds from 2000 to 4000 RPM. The error bars for the measurements using the induction heating at 4000 RPM are shown for clarity. The results from the two configurations are in reasonable agreement with an average difference of about 15%, suggesting that the heat transfer through the rotating heat pipe can be determined from the condenser water jacket. The induction heating configuration was used to characterize the rotating heat pipes in these experiments.

The heat transfer of the tapered heat pipe with the three different fluid loadings are plotted against the temperature difference between the evaporator and condenser in Fig. 7. The wall temperature at the evaporator varied between 40 and 90 °C and the distribution was relatively uniform, with the largest axial difference along the evaporator being less than 10% of the temperature difference between the evaporator and condenser. An increase in the fluid loading decreases the heat transfer, particularly at low rotational speeds. When the fluid loading was increased from 9.2*g* to 18.2*g*, the heat transfer performance remained almost unchanged at 4000 RPM, and decreased approximately

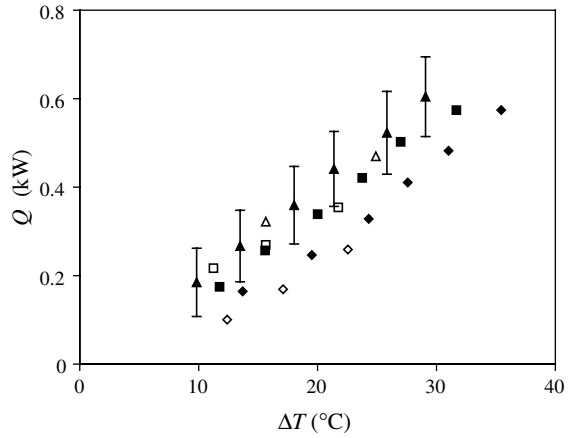

Fig. 6. Change in heat transfer through the heat pipe with temperature difference between the evaporator and the condenser for the tapered heat pipe with 9.2g of water measured with the induction heating at the evaporator at (◆) 2000 RPM, (■) 3000 RPM, (▲) 4000 RPM; measured with the water jacket at the evaporator at (◇) 2000 RPM, (□) 3000 RPM, (△) 4000 RPM.

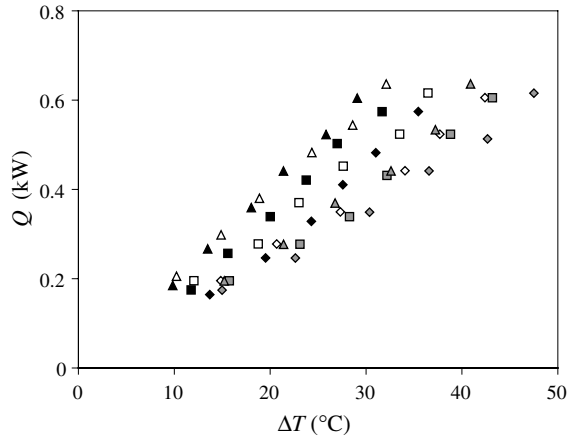

Fig. 7. Change in the heat transfer rate with temperature difference between the evaporator and the condenser for the tapered heat pipe with 9.2g of water at (◆) 2000 RPM, (■) 3000 RPM, (▲) 4000 RPM; with 18.2g of water at (◇) 2000 RPM, (□) 3000 RPM, (△) 4000 RPM; with 32.0g of water at (◈) 2000 RPM, (▣) 3000 RPM, (▲) 4000 RPM.

10% at 3000 and 2000 RPM. Increasing the fluid loading from 9.2g to 32.0g decreased the heat transfer by 20% at 2000 RPM and 30% at 3000 and 4000 RPM. The increase in heat transfer with rotational speed is found to be dependent on the fluid loading. For the lower fluid loadings of 9.2g and 18.2g of water, the heat transfer rate for a given temperature drop increased by approximately 40% when the rotational speed was increased from 2000 to 4000 RPM. This is expected because the component of the centrifugal force parallel to the liquid flow direction in the condenser, $\rho_l\omega^2 R\sin\alpha$, increases with rotational speed resulting in a consequent thinning of the liquid film in the condenser [3]. For the higher fluid loadings, however, the increase in heat transfer with rotational speed is not as significant, with an increase of 20% for fluid loading of 32.0g. This is primarily because at higher fluid loadings the excess fluid pools in the condenser [10], and will be examined in more detail when the measurements are compared to the predictions from the models [10,13]. In all cases, the heat transfer rate increases approximately linearly with the temperature drop ΔT. This indicates that the overall thermal resistance of the heat pipe that is proportional to $(Q/\Delta T)^{-1}$ is approximately constant, and the heat transfer mode is not changing.

The decrease in the heat transfer performance with fluid loading for a cylindrical heat pipe is much more significant than for the tapered case (Fig. 8). In particular, the heat transfer decreased by approximately 40% when the fluid loading was increased from 6.3g to 18.2g, compared to a negligible effect for the tapered case at the higher rotational speeds. An increase of fluid loading in the cylindrical heat pipe increases the thickness of the liquid layer throughout the entire heat pipe, particularly in the condenser, and increases the thermal resistance of the heat pipe for all cases [10]. In a tapered heat pipe, the excess fluid mainly pools in the evaporator, where, as it will be discussed later, it does not affect the overall heat transfer rate significantly. At all these heat fluxes and rotational speeds, the thermal resistance of the cylindrical heat pipes is nearly constant. For the heat pipe with 6.3g of water, the typical wall temperature distri-

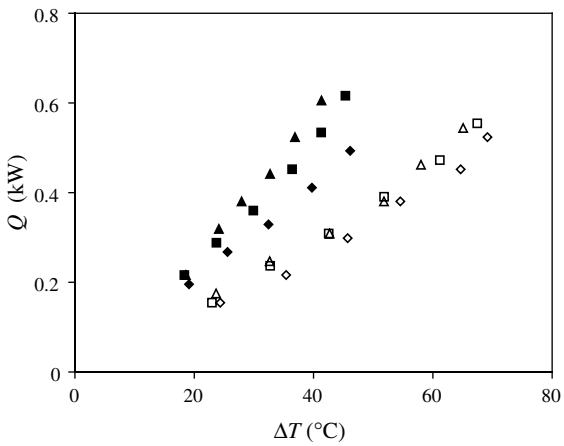

Fig. 8. Change in the heat transfer rate with temperature difference between the evaporator and the condenser for the cylindrical heat pipe with 6.3g of water at (◆) 2000 RPM, (■) 3000 RPM, (▲) 4000 RPM; with 18.2g of water at (◇) 2000 RPM, (□) 3000 RPM, (△) 4000 RPM.

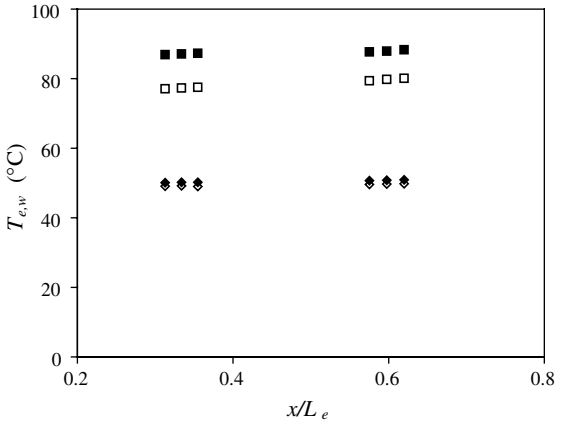

Fig. 9. Measurements of the wall temperature distribution in the evaporator for the cylindrical heat pipe with 6.3*g* of water at (◆) 0.20 kW, 2000 RPM; (■) 0.49 kW, 2000 RPM; (◇) 0.22 kW, 4000 RPM; (□) 0.52 kW, 4000 RPM.

butions at the evaporator were approximately uniform as shown in Fig. 9. However, when the heat transfer was increased beyond 0.5 kW for this heat pipe at 2000 RPM, the evaporator wall temperature increased from approximately 90 °C to above 200 °C, suggesting a dry out condition in the evaporator. A similar phenomenon was not observed in the cylindrical heat pipe with 18.2*g* of water at the same speed range and even higher heat loads. The average heat flux at the evaporator wall was approximately 5×10^4 W m^{-2}, which is significantly below the critical boiling heat flux limit of approximately 10^6 W m^{-2} [16]. Thus, the dry out in this case was likely caused by a lack of working fluid in the evaporator due to the insufficient hydrostatic pressure gradient to drive the liquid flow.

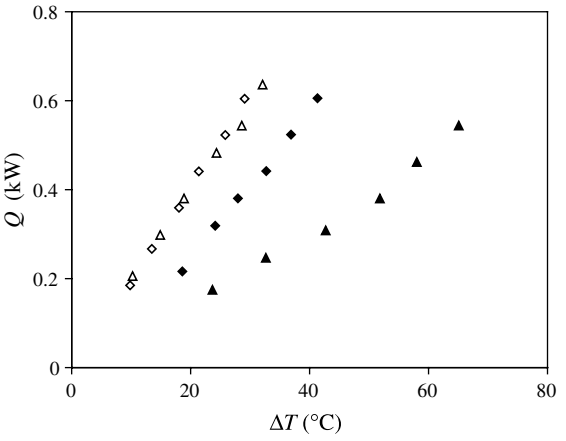

Fig. 10. Comparison of the heat transfer performance at 4000 RPM for the tapered heat pipe with (◇) 9.2*g* of water and (△) 18.2*g* of water, and cylindrical heat pipe with (◆) 6.3*g* of water and (▲) 18.2*g* of water.

The benefit of adding a taper to the condenser was examined by comparing the performance of the tapered and cylindrical heat pipes at a typical speed of 4000 RPM (Fig. 10). The results for the two cases can be evaluated by comparing the overall thermal resistance of the heat pipe. The thermal resistance of the tapered heat pipe with 9.2*g* of water was 70% of that for the cylindrical heat pipe with 6.3*g* of water, and the thermal resistance of the tapered heat pipe with 18.2*g* of water was approximately half that of the cylindrical heat pipe with the same mass of water. In fact, the thermal resistance for the tapered heat pipe with 32.0*g* of water is less than the cylindrical heat pipe with 6.3*g* of water, indicating the addition of the taper significantly enhances the performance of the rotating heat pipe.

4. Comparison between measurements and model predictions

The heat transfer measurements were compared to the predictions from the models proposed by Li et al. [13] and Song et al. [10]. Both use a modified Nusselt film condensation model in the condenser and an adiabatic laminar thin-film model in the adiabatic section. The main difference between the models is at the evaporator, where Li et al. [13] used a modified Nusselt film evaporation model, whereas Song et al. [10] used a mixed convection film evaporation model that reduced to Li et al.'s model when the contribution from natural convection to the evaporation heat transfer was small. The model by Li et al. [13] was also modified here to take into account the effect of excess fluid loading in the heat pipe. The heat transfer was evaluated from the models using a uniform wall temperature boundary condition at the evaporator and condenser. The measurements indicated that the evaporator wall temperature was relatively uniform so that this boundary condition is reasonable, except when dry out appears to occur in the evaporator. The wall temperature at the condenser was not uniform. However, the average value at both sides of the condenser should provide a first approximation for the actual boundary condition that can be used to determine if the models can predict the trends observed in the measurements.

A comparison between the predictions of the model by Song et al. [10] and the measurements for the tapered heat pipe with 9.2*g* and 18.2*g* of water is shown in Fig. 11(a), while the same comparison for the model by Li et al. [13] is shown in Fig. 11(b). The predictions from Song et al.'s model are in reasonable agreement with the measurements, with the model over predicting the measurements by approximately 15%, and seem to capture the correct trends in the results. In particular,

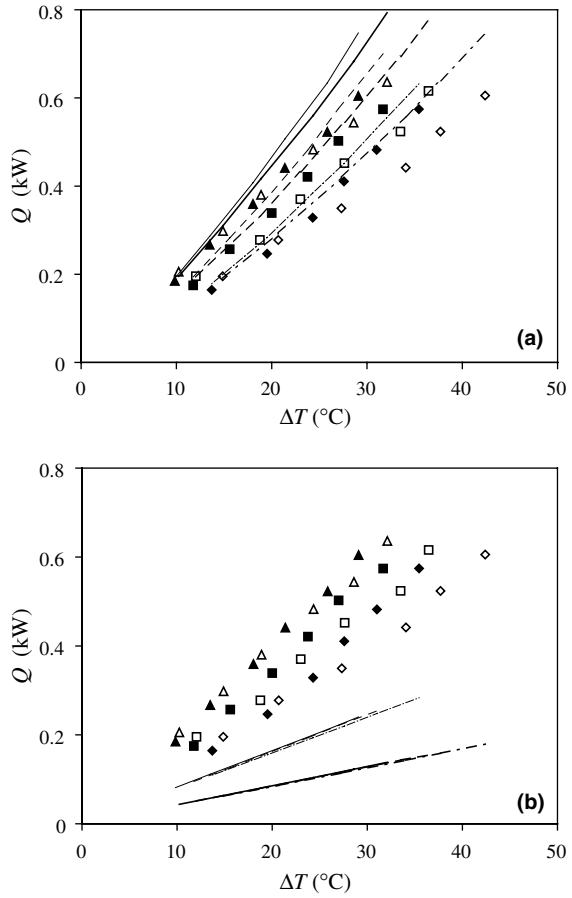

Fig. 11. Comparison of the measured heat transfer performance (presented with symbols) to the predictions (presented with lines) from (a) Song et al.'s model [10] and (b) Li et al.'s model [13] for the tapered heat pipe with 9.2g of water at (◆ and – - –) 2000 RPM, (■ and – – –) 3000 RPM, (▲ and ——) 4000 RPM; with 18.2g of water at (◇ and – - –) 2000 RPM, (□ and – – –) 3000 RPM, (△ and ——) 4000 RPM.

the predicted heat transfer rates increase continually with the rotational speed, and also approximately coincide for the two different fluid loadings, in agreement with the measurements. On the other hand, the predictions from the model of Li et al. [13] under predict the measurements by approximately 60%, and are essentially independent of rotational speed for both fluid loadings in the speed range 2000 to 4000 RPM. The predictions also indicate that the heat pipe performance is strongly dependent on the fluid loading, with a decrease of about 40% when the fluid loading was increased from 9.2g to 18.2g of water. Thus, the performance of the tapered heat pipe with changes in the rotational speed and fluid loading predicted by Li et al. [13] are exactly opposite to those found in the measurements for the parameter range studied here.

The difference in these two models can be further understood by comparing the contributions of the evaporator and condenser to the overall thermal resistance of the heat pipe as shown in Fig. 12. The predictions for the thermal resistance of the condenser from the two models are quite similar and decrease with rotational speed for the same fluid loading. This is not unexpected because the same film condensation model was used in both models. The thermal resistance for the evaporator from the model by Li et al. [13], however, is much larger than that from the model by Song et al. [10]. The evaporator thermal resistance from Li et al.'s model is almost constant with speed because the film thickness profile in the adiabatic section and evaporator becomes more uniform with an increase of rotational speed. The natural convection heat transfer included in Song et al.'s model increases with rotational speed, so the thermal resistance of the evaporator decreases with rotational

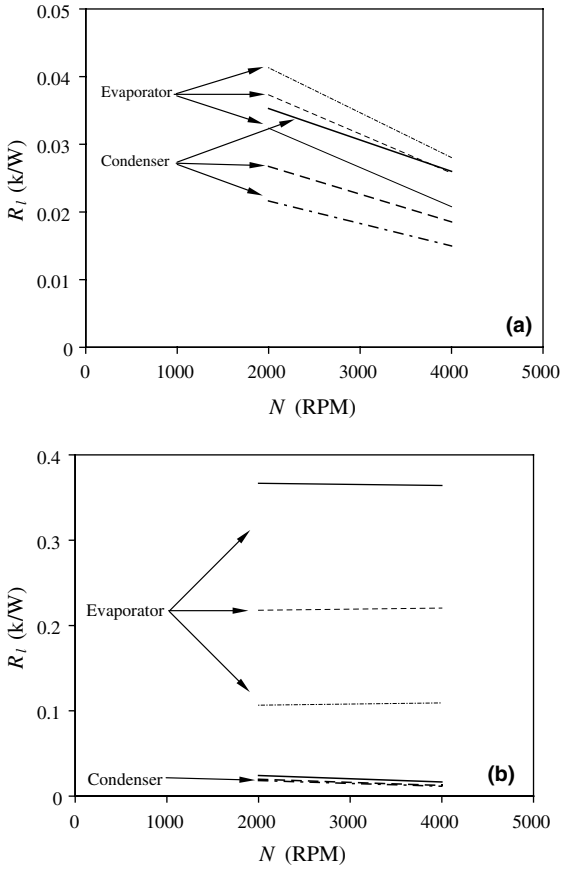

Fig. 12. Change in the thermal resistance of the evaporator (light lines) and the condenser (dark lines) with rotational speed predicted using (a) Song et al.'s model [10] and (b) Li et al.'s model [13] for the tapered heat pipe with 9.2g of water (– - – and – – –); with 18.2g of water (– – – and – – –); with 32.0g of water (—— and ——).

speed in this case. As the fluid loading is increased, the model predicts that the excess fluid initially tends to pool in the evaporator and adiabatic section. However, at higher fluid loadings some fluid begins to pool in the condenser causing the thermal resistance of the condenser predicted by both models to increase. The increase in the film thickness in the evaporator increases the thermal resistance of the evaporator predicted by Li et al.'s model [13], but decreases the thermal resistance predicted by Song et al.'s model [10] because of the inclusion of natural convection. Thus, Li et al.'s model predicted that fluid loading had a significant influence on the performance of the tapered heat pipe, while Song et al.'s model predicted a small change more consistent with the measurements.

The measurements for the cylindrical heat pipe were also compared to the predictions from the two models, as shown in Fig. 13. The predictions from the model proposed by Song et al. [10] are again in better agreement with the measurements. The model under predicts the measurements by 25% and 40% for the heat pipe with 6.3g and 18.2g of water, respectively. The model does seem to accurately predict the change in the performance of the cylindrical heat pipe with changes in both rotational speed and fluid loading. The predictions from the model proposed by Li et al. [13] under predict the measurements by approximately 40% for the heat pipe with 6.3g of water, and 60% for the heat pipe with 18.2g of water. This model, however, does not predict the change in the performance of the heat pipe with speed and significantly over predicts the decrease in the performance as the fluid loading was increased. The difference in the model predictions can again be understood by examining the thermal resistance of the evaporator and condenser predicted from the two models (Fig. 14). The predictions of the thermal resistance of the condenser are again in reasonable agreement from both models. The thermal resistance of the condenser is larger than the evaporator in both models because the flow is driven back to the evaporator by the hydrostatic pressure gradient generated by the centrifugal force so that the film thickness decreases from the condenser to the evaporator. The thermal resistance of the evaporator from the model by Li et al. [13] is much larger than from the model by Song et al. [10], causing the former model to under predict the heat transfer, though by much less than in the tapered heat pipe. Further, the difference in the evaporator thermal resistance seems to explain why Li et al.'s model improperly predicts the change in heat pipe performance with rotational speed. The predicted film thickness becomes more uniform as the rotational speed is increased, causing the thermal resistance of the condenser to decrease for the lower fluid loading and remain unchanged for the higher fluid loading for both models. The predicted thermal resistance of the evaporator from Li et al.'s model increases slightly, offsetting

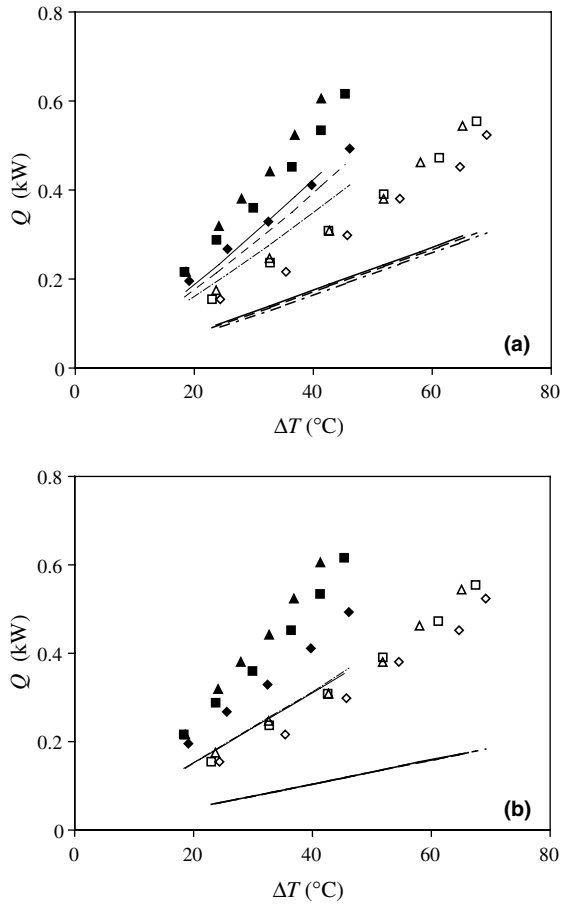

Fig. 13. Comparison of the measured heat transfer performance (symbols) to the predictions (lines) using (a) Song et al.'s model [10] and (b) Li et al.'s model [13] for the cylindrical heat pipe with 6.3g of water at (◆ and — - —) 2000 RPM, (■ and — — —) 3000 RPM, (▲ and ——) 4000 RPM; with 18.2g of water at (◇ and — - —) 2000 RPM, (□ and — — —) 3000 RPM, (△ and ——) 4000 RPM.

the decrease in the thermal resistance of the condenser. The predicted thermal resistance of the evaporator and the overall heat pipe from Song et al.'s model, by contrast, decreases with rotational speed, which is in agreement with the measurements. Similarly, when the fluid loading is increased it causes the film thickness to increase throughout the heat pipe. This leads to an increase of the predicted thermal resistance of the condenser in both models. The thermal resistance of the evaporator predicted by Li et al.'s model also increases resulting in an increase in the overall thermal resistance, which is much larger than in the measurements. Here, again, the thermal resistance of the evaporator predicted by Song et al.'s model is significantly smaller than that of the condenser due to the effect of natural convection in the evaporator. Consequently, the change in the

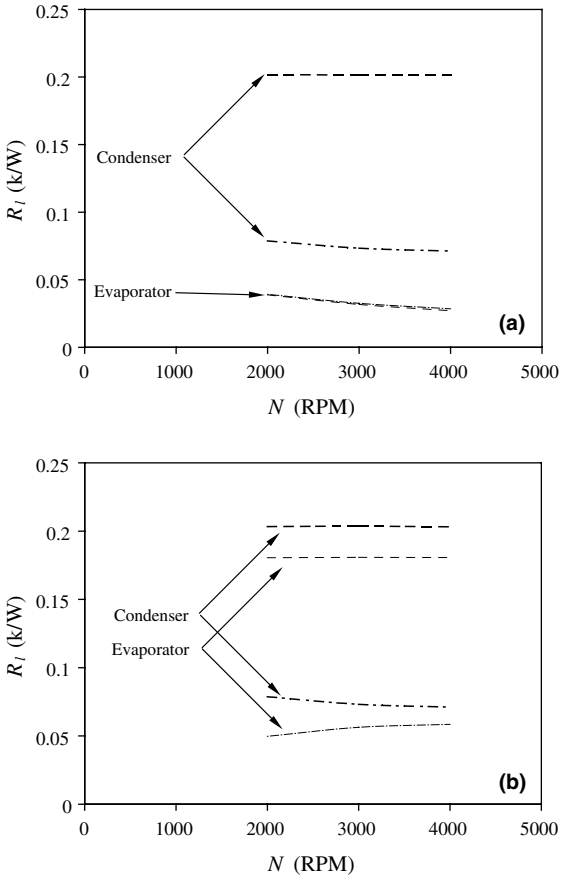

Fig. 14. Change in the thermal resistance of the evaporator (light lines) and the condenser (dark lines) with rotational speed predicted using (a) Song et al.'s model [10] and (b) Li et al.'s model [13] for the cylindrical heat pipe with 6.3g of water (— - — and — - —); with 18.2g of water (— — — and — — —).

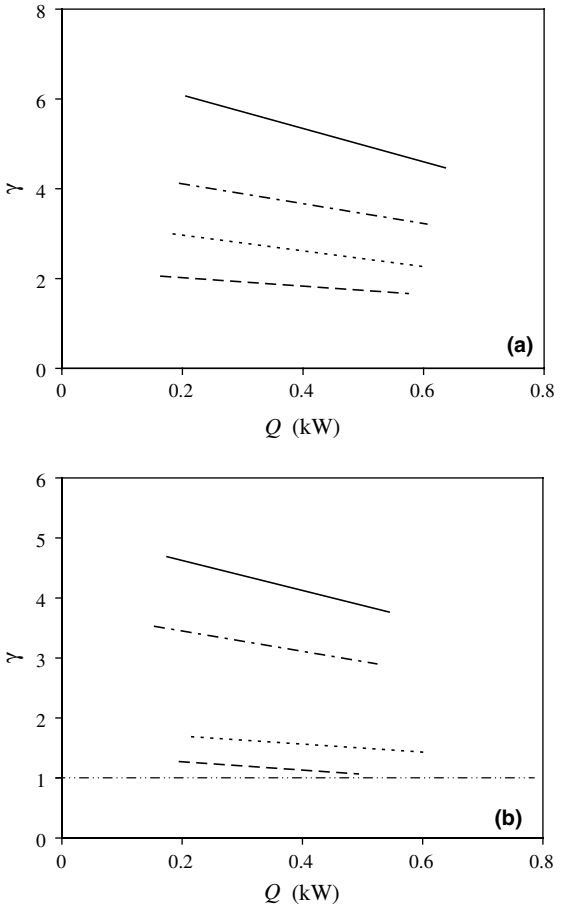

Fig. 15. Change of fluid loading ratio with rotational speed and heat load predicted using Song et al.'s model [10] for (a) the tapered heat pipe with 9.2g of water at (— — —) 2000 RPM, (- - -) 4000 RPM, and with 18.2g of water at (— - —) 2000 RPM, (——) 4000 RPM; and (b) the cylindrical heat pipe with 6.3g of water at (— — —) 2000 RPM, (- - -) 4000 RPM, and with 18.2g of water at (— - —) 2000 RPM, (——) 4000 RPM.

overall resistance is mainly determined by the condenser, and is in better agreement with the measurements.

The predictions of the heat transfer from the model by Song et al. [10] deviate significantly from the measurements for the case where the measured evaporator wall temperature suggests dry out in the evaporator. This can be examined by computing the minimum mass of fluid that must be charged in the heat pipe to ensure the entire evaporator inner surface is covered with liquid. The ratio of the mass of fluid in the heat pipe to the minimum mass of fluid predicted from Song et al.'s [10] model,

$$\gamma = \frac{\text{mass of fluid}}{\text{minimum mass of fluid}} \tag{2}$$

for the different heat pipes in the heat load range investigated here is shown in Fig. 15. For the tapered heat pipe with 9.2g and 18.2g of water, γ varies from 2 to 3 and from 4 to 6, respectively, indicating more than sufficient fluid in both cases. For the cylindrical heat pipe with 6.3g of water, γ varies between 1 and 2. The value is less than 1 at 2000 RPM and a heat rate of 0.5 kW, indicating insufficient working fluid at this condition, and corresponds to that found in the measurements. Thus, the results suggest that this model can predict the conditions for the occurrence of dry out in the evaporator. Further measurements are, however, required for different fluid loadings to determine whether this can be predicted over a wider range of operating conditions. The predictions of γ from Li et al.'s [13] model are generally 5–10% less than those by Song et al. [10] but show the same trend with test conditions.

5. Conclusions

Experiments were performed to investigate the heat transfer performance of axial rotating heat pipes. A heat pipe with an internal cylindrical surface and a heat pipe with a 2° tapered condenser were tested at rotational speeds from 2000 to 4000 RPM with different fluid loadings. The heat transfer rates through both rotating heat pipes increase with an increase in rotational speed and a decrease in fluid loading. The increase in the heat transfer with rotational speed is more pronounced at lower fluid loadings for both the tapered and cylindrical heat pipes. An increase of fluid loading decreases the performance of the cylindrical heat pipe much more than in the tapered heat pipe. The taper in the condenser improves the heat transfer significantly compared to that of the cylindrical heat pipe. The optimum working fluid charge must be determined based on the heat pipe operating conditions to prevent either the occurrence of dry out with a low fluid charge or a reduction of heat pipe performance with a high fluid charge. A comparison between the measurements and predictions from previous models indicates that natural convection is an important heat transfer mechanism influencing the evaporator and the overall heat pipe performance at high rotational speeds. The model proposed by Song et al. [10] that includes the contribution of natural convection in the evaporator can, in general, predict the heat transfer characteristics of the rotating heat pipe.

Acknowledgements

The support of the Natural Sciences and Engineering Research Council (NSERC) of Canada and Pratt & Whitney Canada is gratefully acknowledged.

References

[1] V.H. Gray, The rotating heat pipe—a wickless hollow shaft for transferring high heat fluxes, ASME 69-HT-19, 1969.
[2] G.P. Peterson, An Introduction to Heat Pipes, John Wiley & Sons, Inc., New York, 1994.
[3] T.C. Daniels, F.K. Al-Jumaily, Investigation of the factors affecting the performance of a rotating heat pipe, Int. J. Heat Mass Transfer 18 (1975) 961–973.
[4] F. Song, C.Y. Ching, D. Ewing, Fluid flow and heat transfer modeling in rotating heat pipes, in: 12th International Heat Transfer Conference, France, 2002.
[5] L.L. Vasiliev, V.V. Khrolenok, Heat transfer in rotating heat pipes, in: Proceedings, 7th International Heat Pipe Conference, USSR, 1990, pp. 285–294.
[6] P.J. Marto, L.L. Wagenseil, Augmenting the condenser heat-transfer performance of rotating heat pipes, AIAA J. 17 (6) (1979) 647–652.
[7] P.J. Marto, H. Weigel, The development of economical rotating heat pipes, in: Proceedings, 4th International Heat Pipe Conference, UK, 1981, pp. 709–725.
[8] P.J. Marto, A.S. Wanniarchchi, Influence of internal fins on condensation heat transfer in coaxial rotating heat pipes, in: W.J. Yang (Ed.), Heat Transfer and Fluid Flow in Rotating Machinery, Hemisphere Publishing Co., Washington, DC, 1987, pp. 235–244.
[9] R. Ponnappan, Q. He, J.E. Leland, Test results of a high speed rotating heat pipe, AIAA Paper no. 97-2543, 1997.
[10] F. Song, D. Ewing, C.Y. Ching, Fluid flow and heat transfer model for high-speed rotating heat pipes, Int. J. Heat Mass Transfer 46 (2003) 4393–4401.
[11] R.L. Judd, H. Merte Jr., Evaluation of nucleate boiling heat flux predictions at varying levels of subcooling and acceleration, Int. J. Heat Mass Transfer 15 (1972) 1075–1096.
[12] M.E. Ulucakli, H. Merte Jr., Nucleate boiling with high gravity and large subcooling, J. Heat Transfer 112 (1990) 451–457.
[13] H.M. Li, C.Y. Liu, M. Damodaran, Analytical study of the flow and heat transfer in a rotating heat pipe, Heat Recovery Syst. CHP 63 (1993) 115–122.
[14] W. Nakayama, Y. Ohtsuka, H. Itoh, T. Yoshikawa, Optimum charge of working fluids in horizontal rotating heat pipes, in: D.E. Metzger, N.H. Afgan (Eds.), Heat and Mass Transfer in Rotating Machinery, Hemisphere Publishing Co., Washington, DC, 1984, pp. 633–644.
[15] H.W. Coleman, W.G. Steele, Experimentation and Uncertainty Analysis for Engineers, John Wiley & Sons, New York, 1999, pp. 54–59.
[16] A. Faghri, Heat Pipe Science and Technology, Taylor & Francis, Washington, DC, 1995.